

UNCLASSIFIED

AD NUMBER: AD0248199

LIMITATION CHANGES

TO:

Approved for public release; distribution is unlimited.

FROM:

Distribution authorized to US Government Agencies and their Contractors; Administrative/Operational Use; 31 Dec 1959. Other requests shall be referred to Space and Missile Systems Organization, Los Angeles, CA 90009.

AUTHORITY

SAMSO ltr dtd 3 Mar 1969

UNCLASSIFIED

AD 248 199

*Reproduced
by the*

**ARMED SERVICES TECHNICAL INFORMATION AGENCY
ARLINGTON HALL STATION
ARLINGTON 12, VIRGINIA**



UNCLASSIFIED.

NOTICE: When government or other drawings, specifications or other data are used for any purpose other than in connection with a definitely related government procurement operation, the U. S. Government thereby incurs no responsibility, nor any obligation whatsoever; and the fact that the Government may have formulated, furnished, or in any way supplied the said drawings, specifications, or other data is not to be regarded by implication or otherwise as in any manner licensing the holder or any other person or corporation, or conveying any rights or permission to manufacture, use or sell any patented invention that may in any way be related thereto.

AD NO. **248199**
ASTIA

STL/TR-59-0000-09959

21500

FILE COPY
AFBMD-TR-60-48

819500

**SEMIANNUAL REPORT ON
DEVELOPMENT OF DESIGN CRITERIA
FOR ELASTIC STABILITY OF THIN
SHELL STRUCTURES**

P. Seide
1 JULY - 31 DECEMBER 1959

Contract No. AF 04(647)-309

Prepared for
AIR FORCE BALLISTIC MISSILE DIVISION
AIR RESEARCH AND DEVELOPMENT COMMAND
UNITED STATES AIR FORCE
Inglewood, California

FILE COPY
Return to
ASTIA
ARLINGTON HALL STATION
ARLINGTON 12, VIRGINIA
Air Mail 11555

ASTIA
 RECEIVED
 DEC 28 1959
 TELETYPE UNIT
 TTRK A



SPACE TECHNOLOGY LABORATORIES, INC.
P. O. Box 95001, Los Angeles 45, California

XEROX

**SEMIANNUAL REPORT
ON
DEVELOPMENT OF DESIGN CRITERIA FOR
ELASTIC STABILITY OF THIN SHELL STRUCTURES**

Prepared by

**E. J. Morgan
P. Seide
V. I. Weingarten**

SPACE TECHNOLOGY LABORATORIES, INC.

**P. O. Box 95001
Los Angeles 45, California**

STL/TR-59-0000-09959

Contract No. AF 04(647)-309

1 July - 31 December 1959

Prepared for

**AIR FORCE BALLISTIC MISSILE DIVISION
HEADQUARTERS AIR RESEARCH AND DEVELOPMENT COMMAND
UNITED STATES AIR FORCE
Inglewood, California**

Prepared for
AIR FORCE BALLISTIC MISSILE DIVISION
HEADQUARTERS AIR RESEARCH AND DEVELOPMENT COMMAND
Under Contract AF 04(647)-309

Prepared *E. J. Morgan*
E. J. Morgan

Prepared *P. Seide*
P. Seide

Prepared *V. I. Weingarten*
V. I. Weingarten

Approved *M. V. Barton*
M. V. Barton, Manager
Engineering Mechanics
Department

Approved *G. E. Solomon*
G. E. Solomon, Director
Aeromechanics Laboratory

SPACE TECHNOLOGY LABORATORIES, INC.
P. O. Box 95001
Los Angeles 45, California

ABSTRACT

Experimental data are provided to assist in establishing design criteria for the elastic stability of conical shells and pressure stabilized axially stiffened cylindrical shells. The buckling of a series of Mylar cones and cylinders under axial compression or uniform external pressure was investigated. Some attempts are made to correlate the experimental data obtained. The buckling coefficients of the preliminary results of the initial program (~~see Reference 1~~) * were found to be much lower than the values obtained in subsequent tests. The cones and cylinders in the second series of compression tests had stronger seams so that buckling was not precipitated by initial dimples adjacent to the seam. Test equipment and specimens for the stiffened cylinder investigation were being constructed at the close of the year.

* (Report for Jan-June 1959,
STL/TR-59-0000-00715)

CONTENTS

	Page
I. INTRODUCTION	1
II. CONICAL SHELL PROGRAM	3
A. Testing Technique	3
1. Axial Compression	3
2. External Pressure	3
B. Results and Discussion	5
1. Axial Compression	5
2. Uniform External Pressure	11
C. Conclusions	15
D. Program Plans	16
III. INTERNALLY PRESSURIZED LONGITUDINALLY STIFFENED CYLINDERS	17
REFERENCES	36

ILLUSTRATIONS

Figure		Page
1	Axial Load Test Fixture	4
2	External Pressure Test Fixture	4
3	Cone Buckled by External Pressure	6
4	Variation of C_{exp}/C^* with ρ/t for $\alpha = 0^\circ, 10^\circ, \text{ and } 20^\circ$	8
5	Variation of C_{exp}/C^* with ρ/t for $\alpha = 30^\circ, 45^\circ, \text{ and } 60^\circ$	9
6	Variation of $P/2\pi Et^2$ with Cone Thickness	10
7	Variation of $P/2\pi Et^2$ with Cone Angle	12
8	Comparison of Experimental External Pressure Data with Various Theoretical Investigations	14
9	Critical Stress for Curved Plates as a Function of Internal Pressure and Geometry	19
10	Critical Stress for Curved Plates as a Function of Geometry for Constant Pressure	20
11	Critical Stress for Curved Plates as a Function of Pressure for Constant Geometry	21

TABLES

Table		Page
1	Buckling Data for Conical Test Specimens Under Axial Compression	24
2	Buckling Data for Conical Test Specimens Under External Pressure	30

I. INTRODUCTION

Despite the basic nature of the problems that exist and the considerable effort that has gone into instability investigations over the years, the understanding of shell stability is, at present, limited almost entirely to monocoque cylindrical shells under simple types of loading; and even in these cases, controversy exists regarding the correct interpretation of test data. For conical shells, the theoretical investigations are few, and the available experimental data is quite inadequate.

The purpose of this program is to establish design criteria for the elastic instability of conical shells and pressure stabilized stiffened cylindrical shells. The specific objectives of the experimental work include the determination of:

- a. The design criteria for conical shells under various loading conditions.
- b. The effect of internal pressure on axially stiffened cylindrical shells under similar loading conditions.
- c. The effectiveness of floating rings in stabilizing unpressurized cylindrical shells in various loading conditions.

As described in Project Plan 165-27 (Reference 2), the approach employed in the experimental program consists of a parametric study using Mylar as the specimen material, with corroboration of the Mylar results furnished by tests on larger scale metal specimens.

The results of two experimental stability investigations utilizing Mylar cones are reported herein. The first investigation is on the buckling of Mylar cones and cylinders under uniform compression. The effects on the buckling load of cone angles, radius-thickness ratio, and length-radius ratio were explored in some detail. The results of this investigation are presented in both tabular and graphical form and some tentative correlations of the data and conclusions are made. The second investigation concerns the stability of Mylar cones and cylinders under uniform external pressure.

In the same period, test fixtures and specimens were designed and constructed for the internally pressurized stiffened cylinder program. A description of these is given, and the results of some theoretical investigations to aid in guiding the experimental program are discussed.

II. CONICAL SHELL PROGRAM

In the present program period, the axial compression tests outlined in Reference 1 were completed. In addition, tests were made on conical shells subjected to uniform external hydrostatic pressure. The results of these tests are given herein.

A. Testing Technique

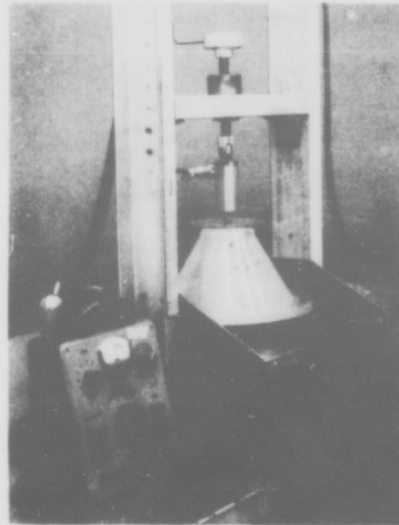
1. Axial Compression

Some modifications of the testing technique were made to insure greater accuracy of the results. In Reference 1, it was noted that an initial dimple appeared in the seam for almost all of the cones. Subsequent tests revealed that for some of the specimens, the dimple grew as the load was increased until the cone collapsed. On these cones the well known diamond shaped buckles never appeared, and the collapse load was usually very low. It was found that a 1-1/4-inch seam overlap, rather than the 3/8-inch overlap used in the tests of Reference 1, eliminated this type of premature failure.

The test fixture was unchanged except for the use of an electronic load cell (Figure 1) rather than the load rings used previously. The test procedure was changed, however, to eliminate the effects of eccentricity of loading. The first axial compression test on any cone was performed with the steel ball and loading plate centrally located. At buckling, the location of the first buckle was recorded. The loading plate and steel ball were then moved 1/4-inch away from the buckle, along the diametral line through the buckle. This procedure was continued until a maximum compressive load was obtained.

2. External Pressure

For cones under external pressure, the following technique was used. The specimen was first fixed in the upper clamping fixture and then placed on the inner portion of the lower clamping fixture which had been raised approximately two inches above the base of the loading fixture by two parallel blocks. This prevented the bottom of the cone from pressing on the base of the loading fixture. The outer portion of the clamp was then placed over the cone



5873

Figure 1. Axial Load Test Fixture.



5874

Figure 2. External Pressure Test Fixture.

and brought down loosely on top of the inner lower clamp. This procedure was developed after it was discovered that if the lower clamps were fastened by screws, dimples appeared and caused premature buckling.

The cones were loaded in the test jig shown in Figure 2. Differential pressure was applied by evacuating the interior of the cone using a vacuum cleaner motor. An alcohol-kerosene manometer was used to measure the pressure differential.

The vacuum was increased slowly by increasing the speed of the vacuum cleaner motor with a Variac until the cone was fully buckled. At this point, the alcohol-kerosene manometer was read and the buckling pressure obtained through the use of the previously determined calibration factor. Each run was repeated four times. The number of buckles around the circumference was recorded in addition to the buckling pressure. A picture of a typical buckled cone appears in Figure 3.

B. Results and Discussion

1. Axial Compression

In Reference 1 it was explained that small deflection theory for the buckling of conical frustums under axial compression gives the buckling load as

$$P_{\text{cone}} = P_{\text{cyl}} \cos^2 \alpha \quad (1)$$

where

P_{cyl} = the theoretical axial buckling load
of a long cylinder ($0.6 \times 2\pi Et^2$)

α = Semivertex angle of the cone

A modification of this formula to take into account the well-known discrepancy between theory and experiment for axial compression of cylinders was suggested as

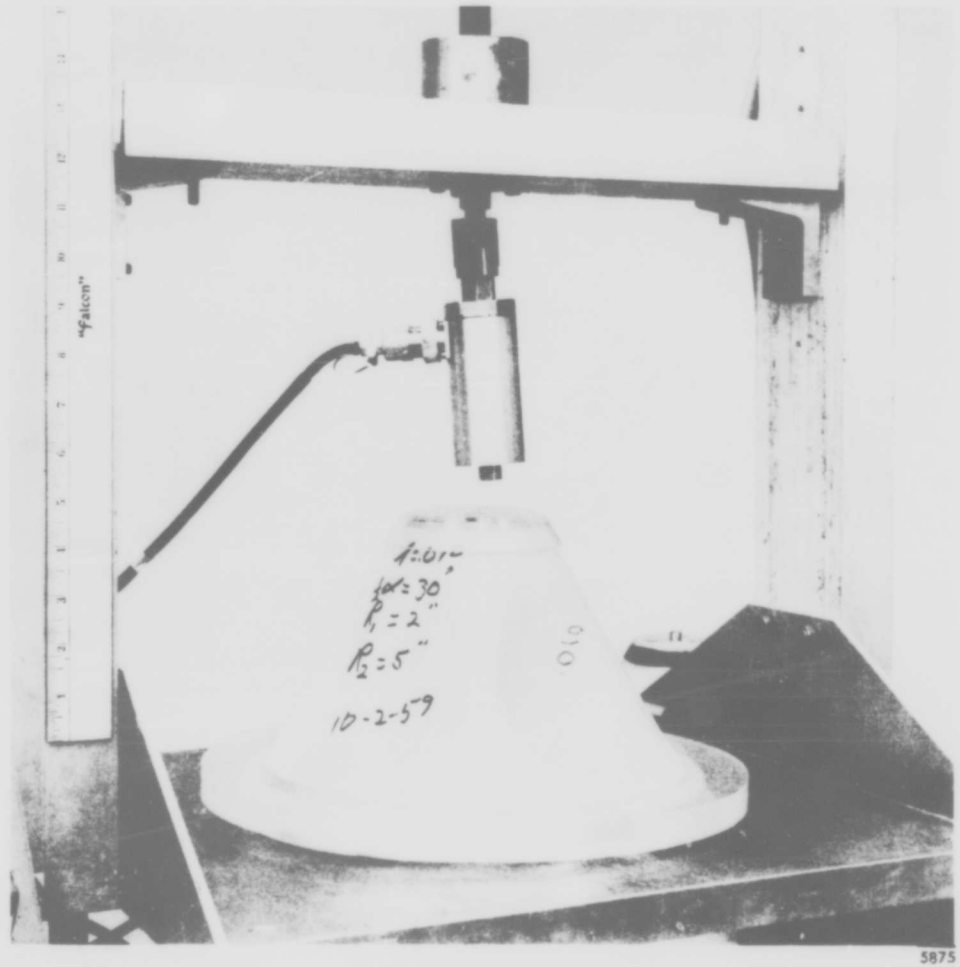


Figure 3. Cone Buckled by External Pressure.

$$P_{\text{cyl}} = (C^*) 2\pi Et^2 \quad (2a)$$

where C^* is an empirically determined coefficient for cylinders (Reference 1),

$$C^* = 9 \left(\frac{t}{\rho} \right)^{0.6} + 0.16 \left(\frac{\rho}{l} \right)^{1.3} \left(\frac{t}{\rho} \right)^{0.3} \quad (2b)$$

where ρ = average radius of curvature of the cone
 l = slant length

The dimensions of the cones were chosen so as to provide some basis for testing this hypothesis. In a number of cones having the same semivertex angle, the value of ρ/l was held constant and ρ/t was varied. The results of the tests carried out on the various cylinders and cones are given in Table 1, where experimental values of C given by

$$C_{\text{exp}} = \frac{P}{2\pi Et \cos^2 \alpha} \quad (3)$$

are compared with the value of C^* computed from Equation (2b).

Two phenomena can be noted immediately from an examination of the last column of Table 1, where the ratio C_{exp}/C^* is listed. One is that for cones of all angles, including cylinders, the ratio of experimental and predicted values of C appears to increase as the average radius-thickness ratio increases. The other is that the ratio increases as the semivertex angle increases. These two effects are shown graphically in Figures 4 and 5. The increase with radius-thickness ratio is seen more clearly by isolating the results of these tests for which only the thickness was varied. Thus, in Figure 6, values of $P/2\pi Et^2$ are plotted as a function of thickness. Also given are the values obtained from Equation (2b) multiplied by $\cos^2 \alpha$. It can be seen that the experimental buckling coefficient $P/2\pi Et^2$ does not show as much variation with thickness as it predicted by Equation (2b). Indeed, if one takes all the scatter into account the results indicate, on the average, no variation with radius-thickness ratio.

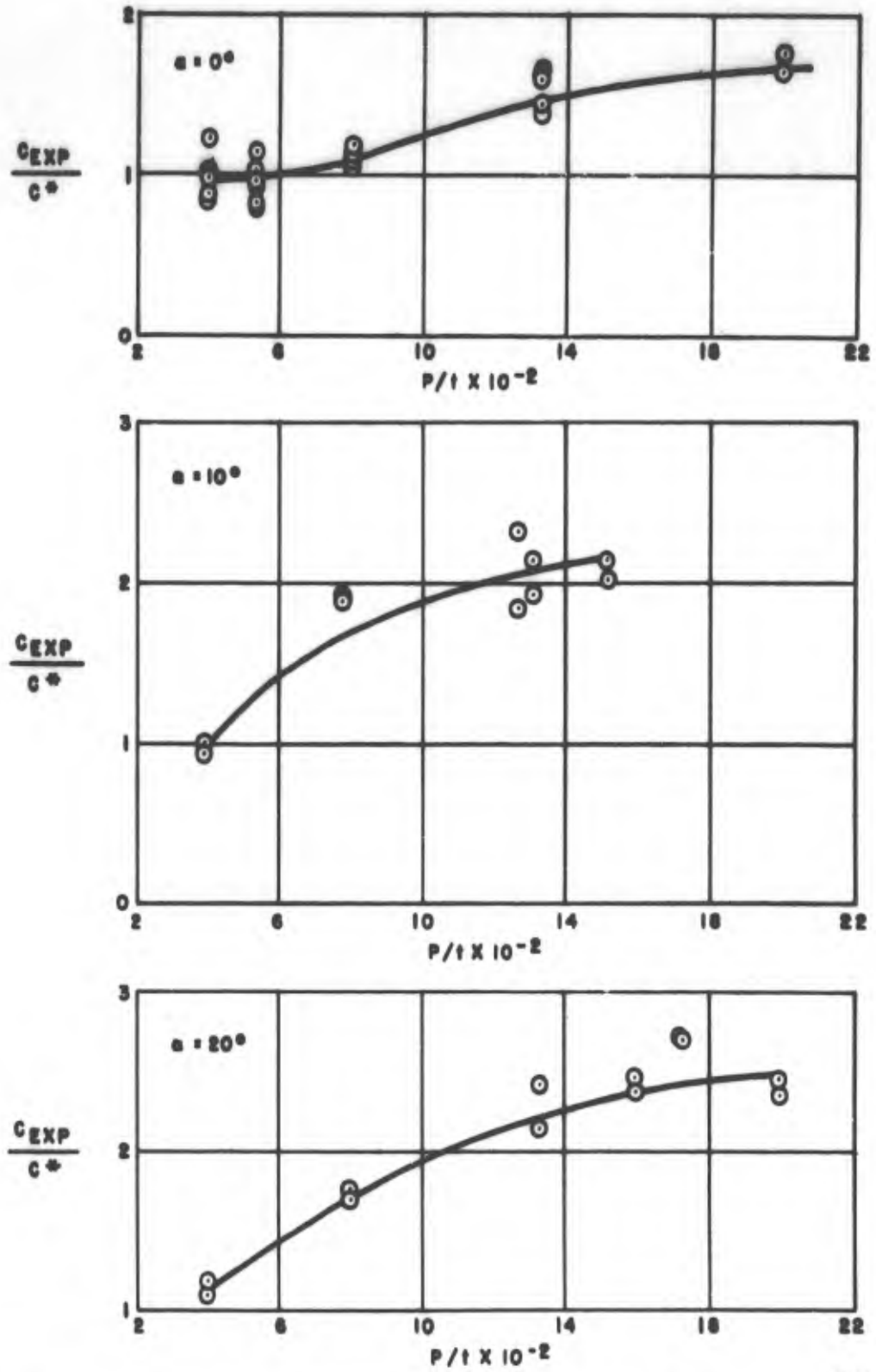
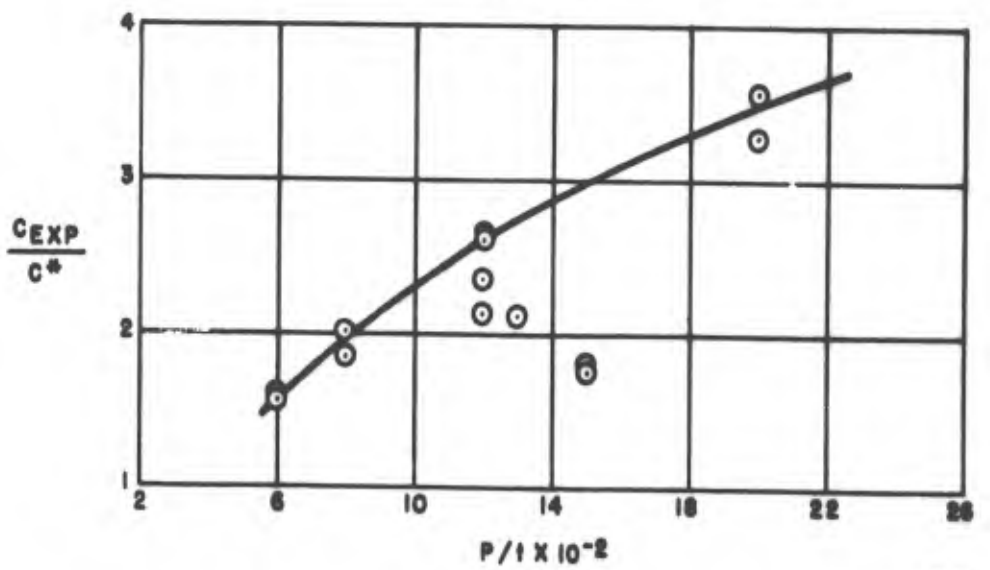
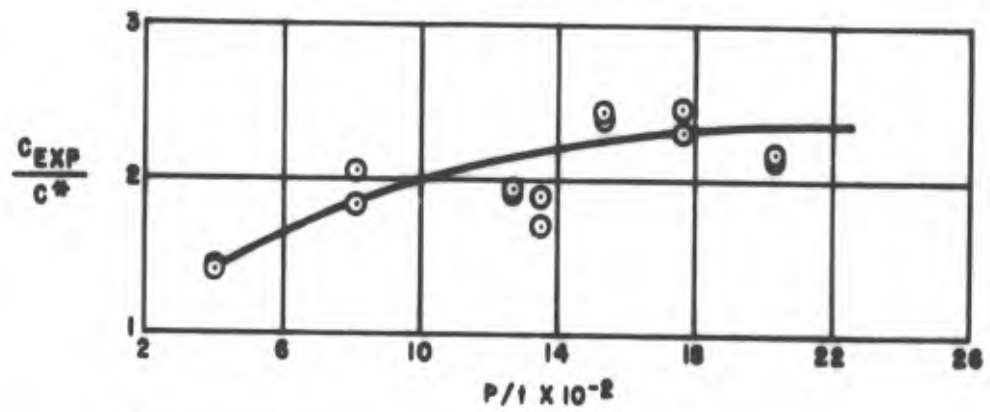
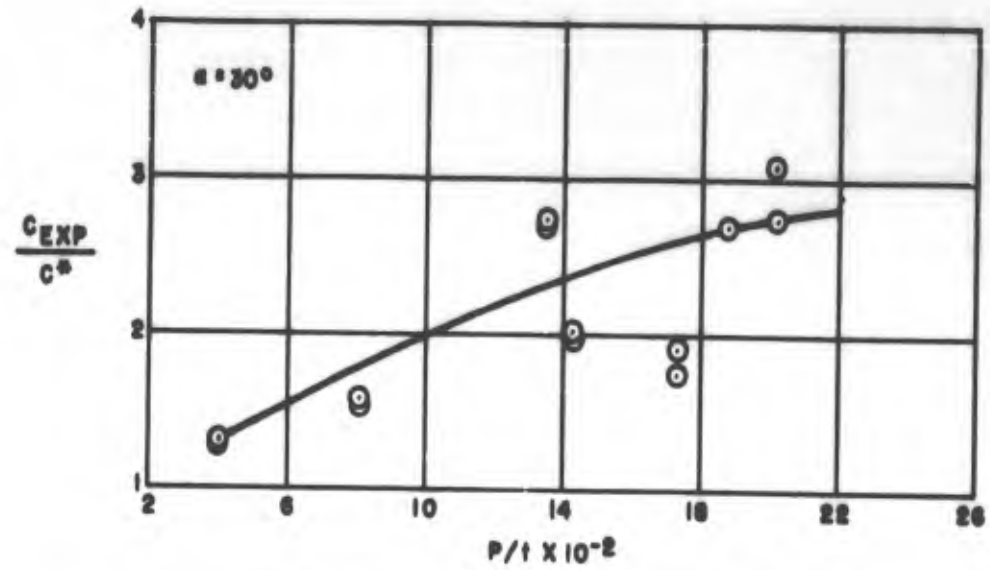


Figure 4. Variation of C_{exp}/C^* with ρ/t for $\alpha = 0^\circ, 10^\circ,$ and 20° .



7084

Figure 5. Variation of C_{exp}/C^* with ρ/t for $\alpha = 30^\circ$, 45° , and 60° .

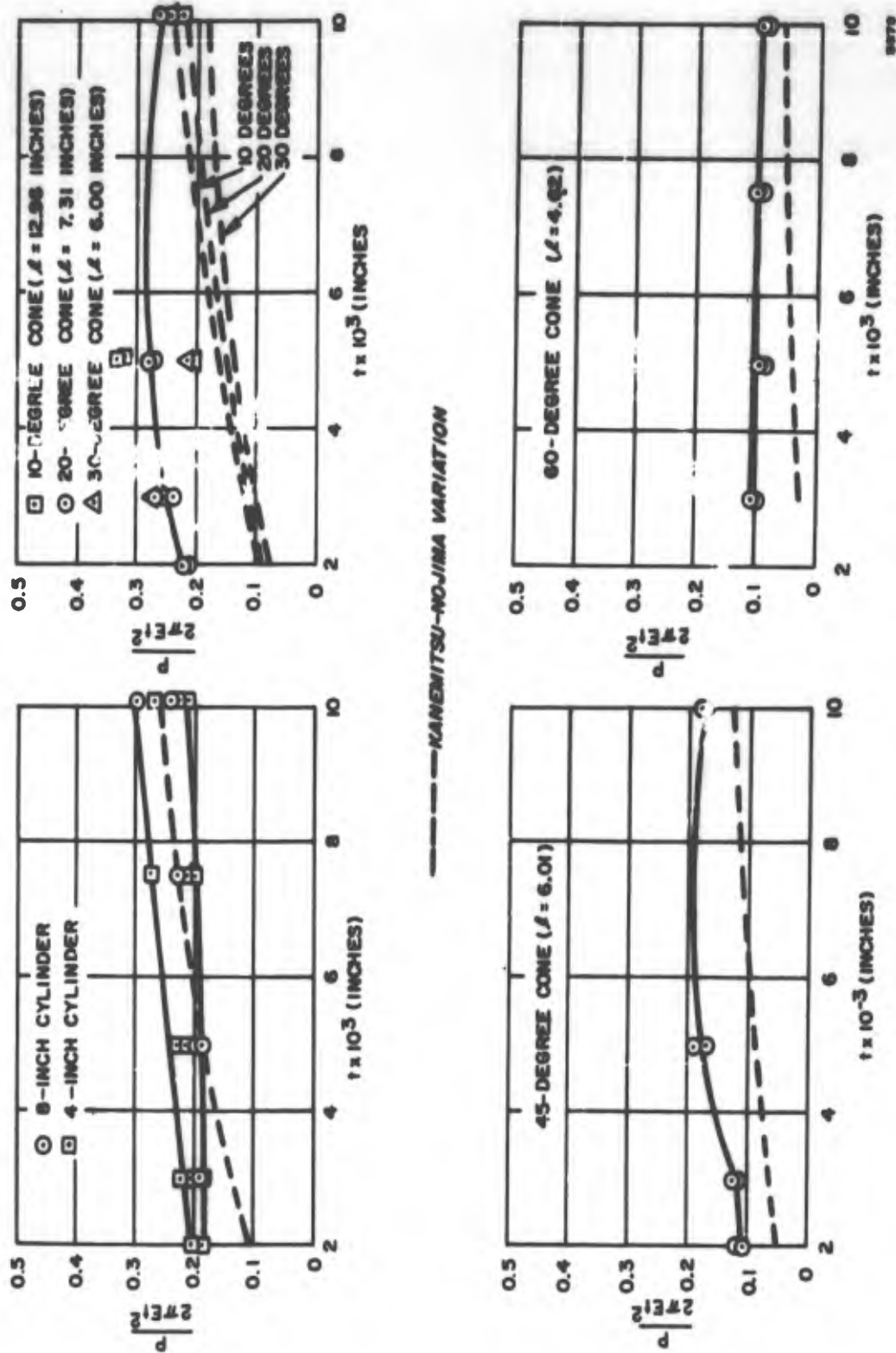


Figure 6. Variation of $P/2\sigma Et^2$ with Cone Thickness.

It is somewhat difficult to explain these occurrences. One explanation might be that the lack of significant variation with radius-thickness ratio is due to the Mylar cones being more nearly ideal than is possible with metal shells. Another, and more likely, explanation is that the number of tests for each radius-thickness ratio is insufficient to yield any statistical variation. The increase of the buckling coefficient ratio with semivertex angle is likewise difficult to explain. A possible explanation might be the stiffening effect of wedging the cones against the lower clamps when loaded in axial compression. On the other hand, this phenomenon may be entirely characteristic of conical shells and might be expected if a large deflection analysis of the buckling process were available.

A more significant correlation of the data is obtained when the values of $P/2\pi Et^2$ are plotted, as a function of the semivertex angle α , without regard to length or thickness (Figure 7). In this plot, the scatter band is about ± 20 percent wide about the mean value for each angle, which is quite good considering the amount of scatter that is usually associated with shell experiments. The trend of the mean of the results is in good agreement with the $\cos^2 \alpha$ variation predicted by small deflection theory, although it should be noted that the results are somewhat lower than the predicted variation for angles near 0 and somewhat higher for angles above 45 degrees. For angles between 15 and 45 degrees, the mean buckling coefficients are quite well represented by the curve

$$\frac{P}{2\pi Et^2} = 0.3 \cos^2 \alpha \quad (4)$$

which is about half of the value predicted by small deflection theory. Confidence in the validity of the experimental values for Mylar is enhanced by the fact that the data of Reference 3 for aluminum cones fell within the scatter band. The point above the scatter band was obtained from Reference 4, in which tests on aluminum cones under axial compression and external pressure are reported. The average radius-thickness ratio for the cones represented by this point was 152 which is well below the range of the Mylar cones.

2. Uniform External Pressure

For conical shells under uniform external pressure, many theoretical investigations are reported in the literature. These are surveyed in Reference 5

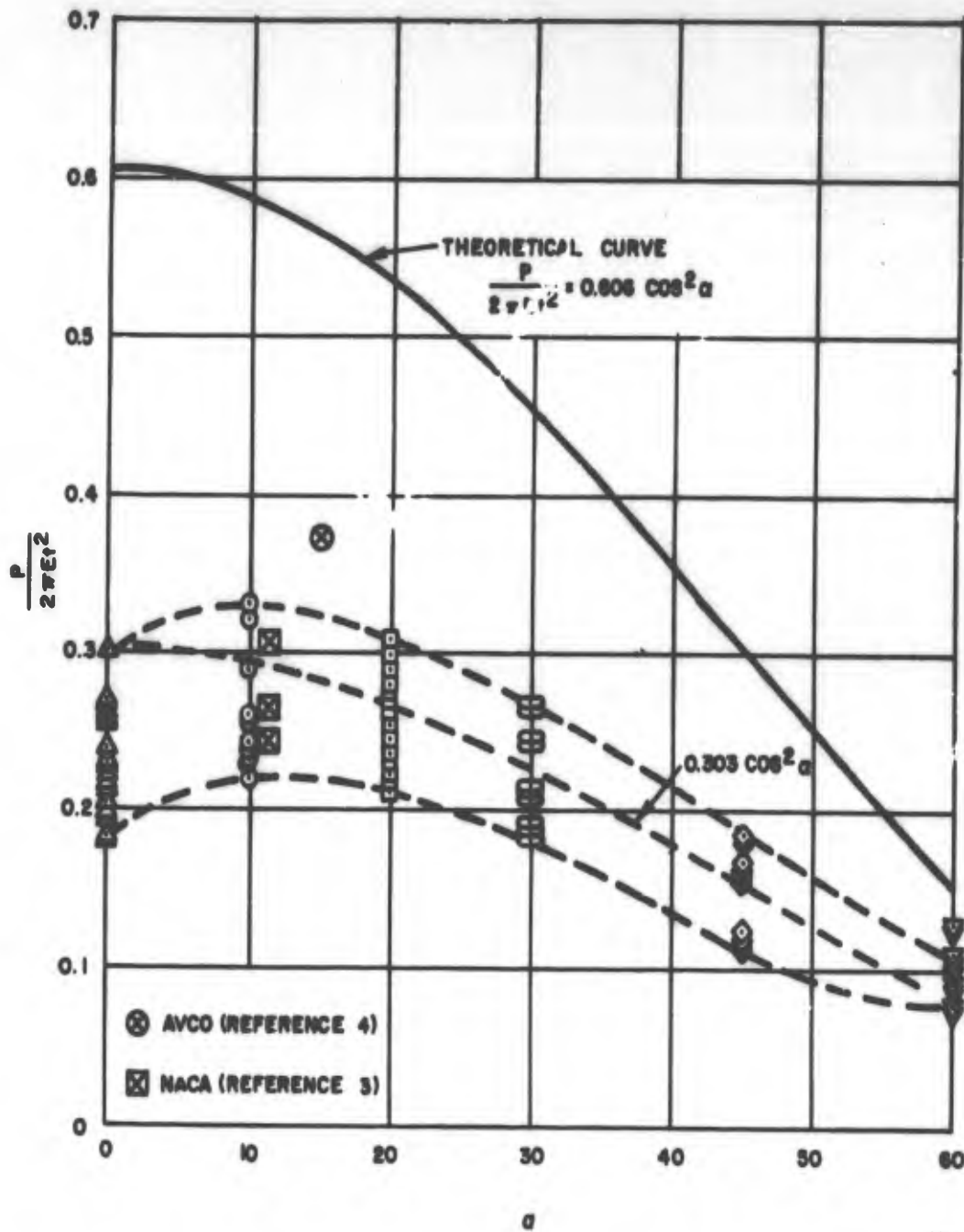


Figure 7. Variation of $P/2\pi Et^2$ with Cone Angle.

where it is shown that most of the significant investigations indicate that the critical pressure of the conical shell is related to the critical pressure of the equivalent cylinder defined previously for axial compression.

The experimental critical pressures p obtained from tests carried out on Mylar cones are given in Table 2. The computed values of critical pressure \bar{p} were obtained by modifying the formula for cylinders given in Reference 6 to read

$$\bar{p} = \frac{\pi^2}{12(1-\nu^2)} E \left(\frac{t}{p}\right)^3 \left(\frac{p}{l}\right)^2 \frac{1}{\frac{1}{2} + \left(\frac{\bar{n}}{\pi p}\right)^2} \left\{ \left[1 + \left(\frac{\bar{n}l}{\pi p}\right)^2 \right]^2 + \frac{12(1-\nu^2)}{\pi} \frac{\left(\frac{l^2}{pt}\right)^2}{\left[1 + \left(\frac{\bar{n}l}{\pi p}\right)^2 \right]^2} \right\} \quad (5)$$

The number of circumferential buckles \bar{n} was varied until a minimum value of \bar{p} was obtained. The computed number of buckles given in the last column of Table 2 was obtained by multiplying the value of \bar{n} yielding minimum critical pressure by $\cos \alpha$, as suggested in Reference 5.

In Figure 8, the values of p/\bar{p} for the cones tested are plotted as a function of cone taper ratio and are compared with various available theoretical results. It can be seen that on the average, p/\bar{p} is insensitive to taper ratio and is equal to unity, thus verifying the approximation given by Niordson. The scatter band is about ± 20 percent, the same as for conical shells in axial compression and, for the most part, lies between the theoretical band defined by the theories of Seide and Bijlaard. On the same figure, experimental results for aluminum and other plastic cones, obtained from References 4 and 7, are plotted and indicate the same behavior. The points plotted above the theoretical band may be explainable by deviations of the actual modulus of elasticity from the average values used in computing p . Another explanation may be afforded

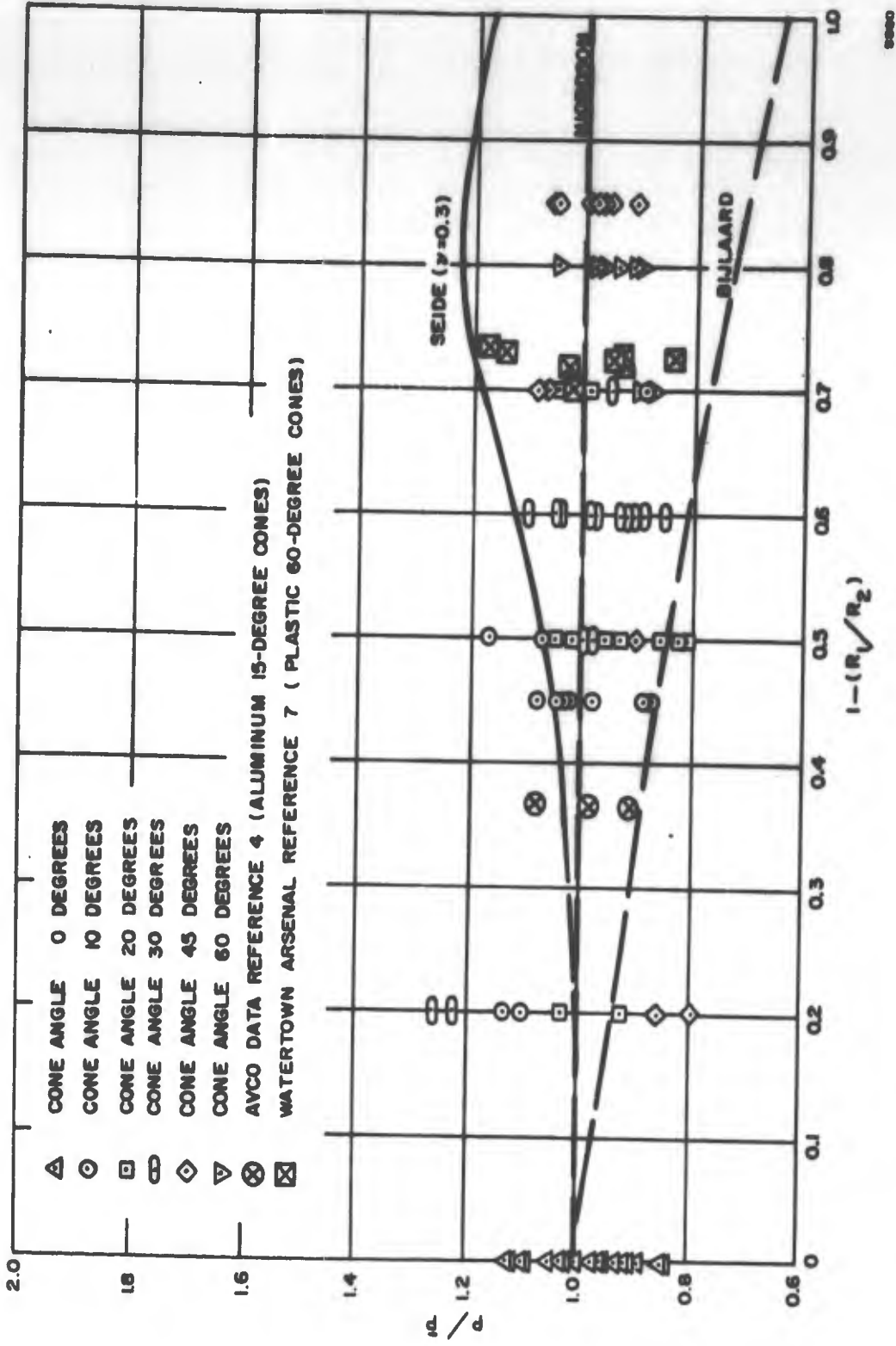


Figure 8. Comparison of Experimental External Pressure Data with Various Theoretical Investigations.

by the difficulty in determining the buckling pressure for some cones for which the formation of buckles was characterized by a slow progressive process rather than a sudden appearance of buckles.

The number of buckles is similarly in fair agreement with the Niordson approximation, although the computed results are, for the most part, higher than those obtained experimentally. A possible explanation for this discrepancy may be the stiffening effect of the 1-1/4-inch seam which would affect the buckle pattern in its vicinity. Thus, some of the buckles may have been "washed out" in the vicinity of the seam.

C. Conclusions

1. The good agreement with the results of investigations involving some other materials indicates, at least tentatively, that Mylar is adequate as a material for buckling tests.

2. The axial compression tests confirm the predicted variation of $P/2\pi Et^2$ with semivertex angle, the value for semivertex angles varying from 15 to 45 degrees being given by

$$\frac{P}{2\pi Et^2} = 0.3 (1 \pm 0.2) \cos^2 \alpha \quad (6)$$

Equation (6) is unconservative for angles near 0 degrees, where the coefficient, multiplying $\cos^2 \alpha$, varies from 0.18 to 0.3, and is conservative for angles near 60 degrees, where the coefficient varies from 0.3 to 0.44. The use of Equation (3) for the buckling load coefficient will be conservative for most cones and may be justified if the manner of load introduction is uncertain. However, the amount of conservatism indicated by the present test results is quite high for the larger semivertex angles.

3. Although the scatter of the test results for a given cone angle is in general satisfactory, certain areas show excessive scatter and will be the subject of additional tests.

4. The critical uniform hydrostatic buckling pressure for a conical shell is shown by the tests to be adequately defined by the approximate formula

$$P \approx \frac{0.92 E}{\frac{l}{\rho} \left(\frac{\rho}{t} \right)^{5/2}} \quad (7)$$

where l = slant length of the cone

ρ = average radius of curvature

t = thickness

The scatter in the results is approximately ± 20 percent about the mean value given by Equation (7).

5. The test results indicate the need for a large deflection theory for buckling of conical shells, possibly to explain the increase in axial buckling load coefficient with semivertex angle, and the discrepancy of Equation (7) with the results of the theory of Reference 5.

D. Program Plans

To increase the confidence in the results of Mylar test specimens, a series of tests utilizing steel conical shells has been planned. During the next program period, work will continue on the interaction between axial compression and external or internal pressure utilizing Mylar specimens. Additional axial compression testing is planned in order to check scatter points in certain areas such as $\alpha = 30^\circ$, $\rho/t = 1200^\circ$ to 1800, $\alpha = 45^\circ$, $\rho/t = 1300$, and $\alpha = 60^\circ$, $\rho/t = 1200$ and 1600.

III. INTERNALLY PRESSURIZED LONGITUDINALLY STIFFENED CYLINDERS

It has been established that the critical buckling stresses for pressurized cylinders are greater than those for unpressurized cylinders. Since the strength-weight ratio of efficiently stiffened shells exceeds that of unstiffened ones it is believed that weight saving is possible in many practical cases by combining pressurization and stiffening. The purpose of this program is to determine what advantages can be derived from this combination, and to set up criteria for the design of efficient structures. The first phase of the program consists of an experimental study of the influence of internal pressure on the local and general instability of longitudinally stiffened cylinders under axial compression.

Dimensional analysis indicates that the probable most important nondimensional parameters are

$$\frac{\sigma_{cr}}{E_s} = \text{Function} \left[\frac{R}{t}, \frac{b}{t}, \frac{L}{b}, \frac{t_e}{t}, \frac{(EI)_L}{bD}, \frac{(GJ)_L}{bD}, \frac{pR}{Et} \right] \quad (8)$$

where the notation is

A_L	cross-sectional area of stiffener
b	circumferential width of panel between stiffeners
D	flexural stiffness of skin
E_L	Young's modulus of stiffener material
E_s	Young's modulus of cylinder material
$(EI)_L$	flexural stiffness of stiffeners
$(GJ)_L$	torsional stiffness of stiffeners
L	length of cylinder
p	internal pressure
R	radius
t	skin thickness
t_e	effective thickness, $t_e = t + E_2/E_s A_L/b$
σ_{cr}	average critical stress

The ratios of bending and torsional rigidity of the stiffeners to the flexural stiffness of the skin are the same parameters used in the analysis of a plate with elastic edge supports. For plates, the buckling stress deviates from that for a clamped plate only when these ratios are very low. For the problem under consideration, these ratios are relatively high when the stiffeners are required to remain straight (References 8 and 9). Therefore, because of the similarity between these two cases, it is likely that if the stiffeners remain straight when the panels buckle, the panels will behave as if clamped along their edges. This case is difficult to analyze, however, and an alternate investigation of the effect of pressure on cylinder panels was made using the theory of Reference 6, assuming the long edges to be simply supported. The results of the analysis are given by

$$\bar{\sigma}_{cr} - \frac{\bar{p}}{m^2} = \frac{m^2 \beta}{(m^2 + 1)^2} + \frac{(m^2 + 1)^2}{12(1 - \nu^2) \beta m^2} \quad (9)$$

in which

$$\bar{\sigma}_{cr} = \left(\frac{\sigma_{cr}}{E} \right) \left(\frac{R}{t} \right), \quad \bar{p} = \left(\frac{p}{E} \right) \left(\frac{R}{t} \right)^2, \quad \beta = \left(\frac{1}{4\pi^2} \right) \left(\frac{b^2}{Rt} \right)$$

The solution of this equation, after minimizing with respect to m , is illustrated in Figure 9.

In the figure, as b^2/Rt becomes very large, σ_{cr} approaches the theoretical value for the unstiffened cylinder, whereas for low values of b^2/Rt , σ_{cr} is significantly greater than the unstiffened cylinder value. For comparison with this small deflection solution, some experimental data (References 10, 11, 12) for curved panels are plotted in Figures 10 and 11. In Figure 10, the critical stress is plotted as a function of shell geometry parameters for two pressures. As might be anticipated from the work of References 13, 14 and 15, the experimental points for the unpressurized shells are well below theory. However,

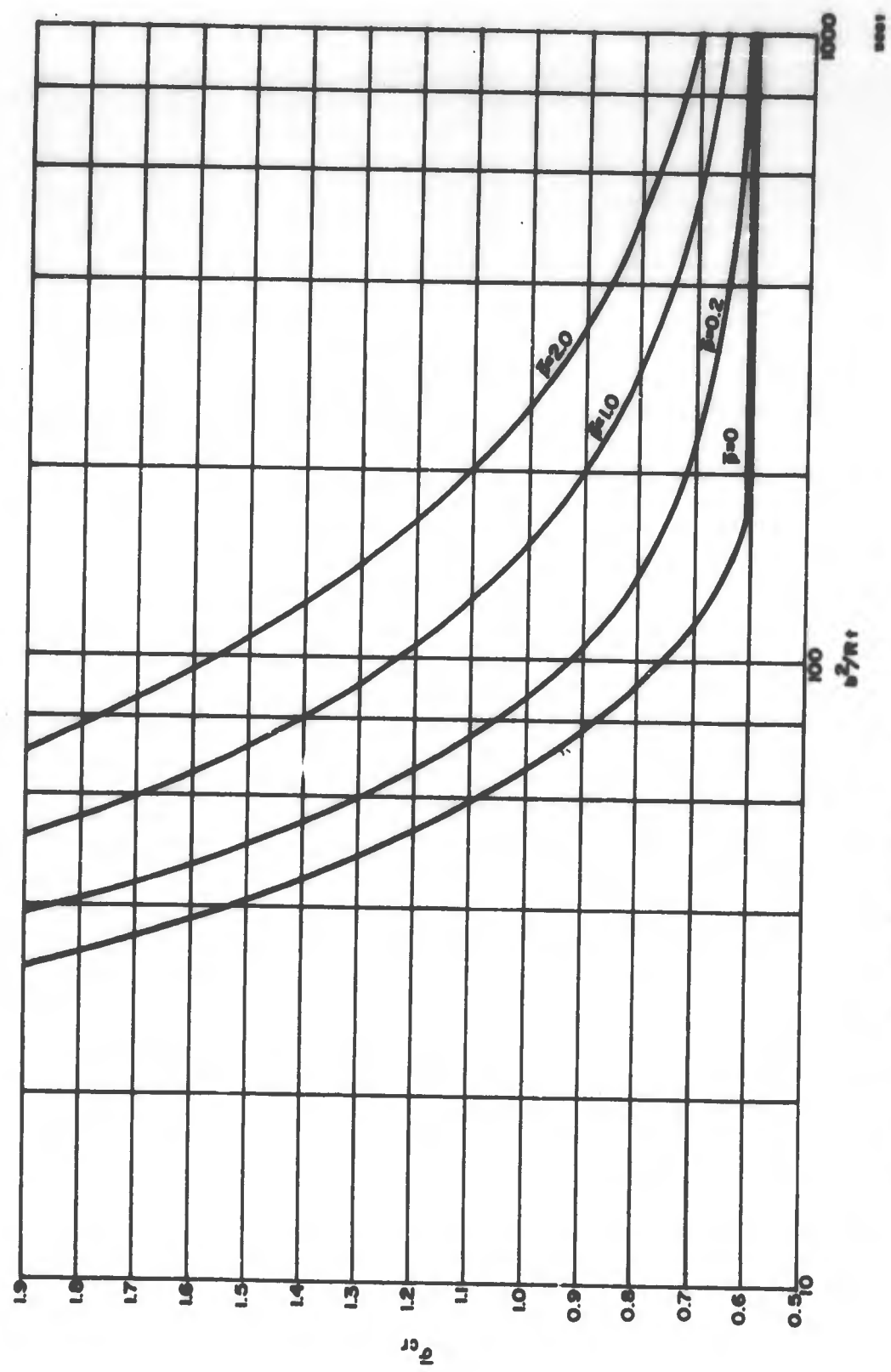


Figure 9. Critical Stress for Curved Plates as a Function of Internal Pressure and Geometry.

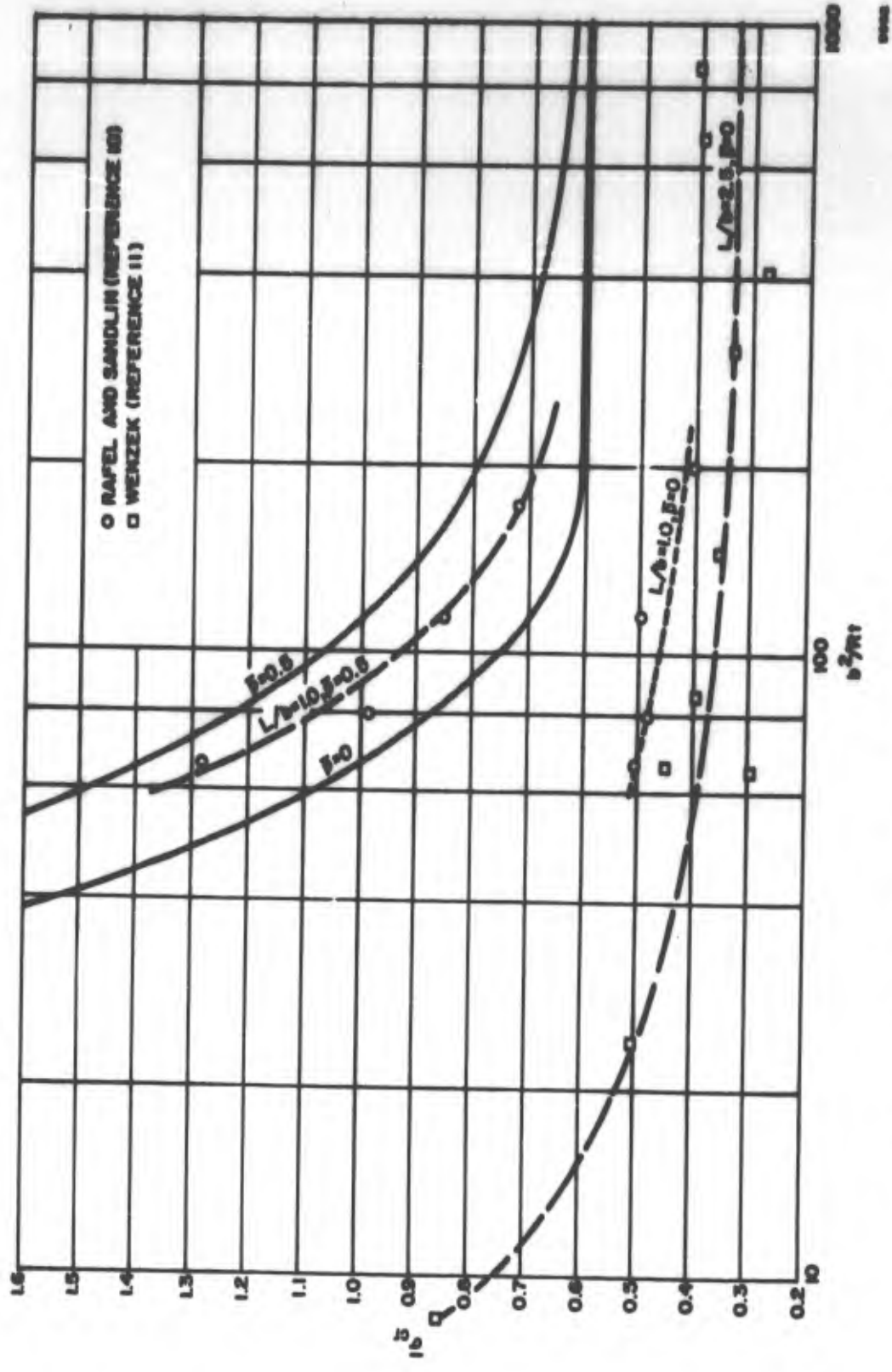


Figure 10. Critical Stress for Curved Plates as a Function of Geometry for Constant Pressure.

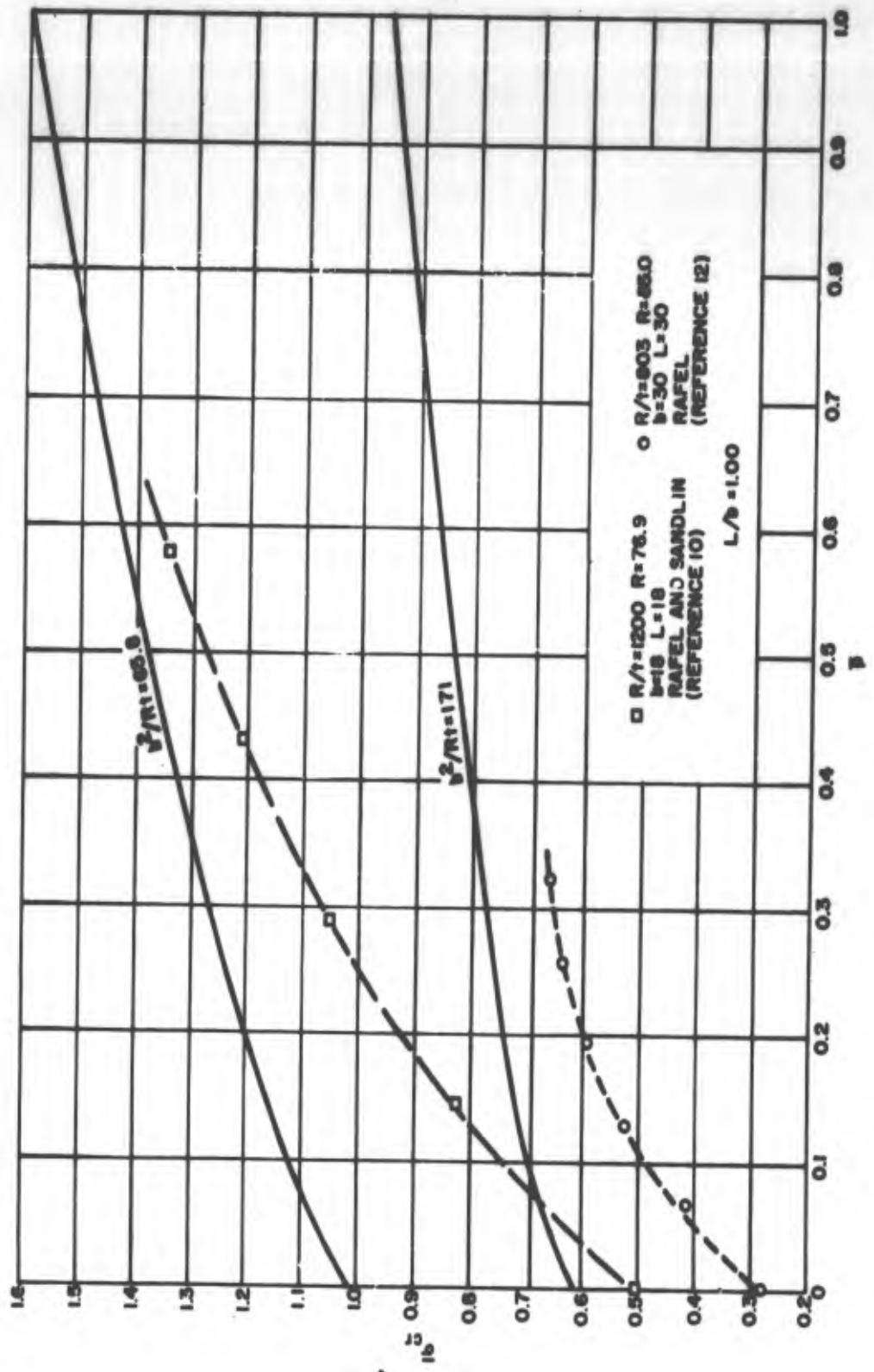


Figure 11. Critical Stress for Curved Plates as a Function of Pressure for Constant Geometry.

these data for $\bar{p} = 0.5$ are in much better agreement with the theoretical results. The trend for the critical stress to approach the theoretical value as the internal pressure increases is illustrated in Figure 11.

A more complete parametric study has been proposed using Mylar as the cylinder material. The excellent recovery properties of Mylar enable each specimen to be tested several times; thus permitting each cylinder to be tested over a range of internal pressures. A similar material, cellulose acetate or polystyrene, will be used for the stiffeners.

The first series of tests have been designed to determine what influence the stiffener size will have upon the buckling stress of a given panel. This series of specimens will be identical with the exception of stiffener cross sections. A large range of flexural and torsional rigidities will be covered. The parameters selected for this series are

$$\begin{aligned} R &= 4.0 \\ t &= 0.005 \\ L &= 8.0 \\ N &= 30 \end{aligned}$$

$$\frac{b_e^2}{Rt} = 25.4$$

$$\frac{(EI)_L}{bD} = 500 - 2500$$

$$\frac{(GJ)_L}{bD} = 20 - 800$$

If the analogy with the plate on elastic supports is correct, then little difference should be observed for this range of stiffness. If the assumption of clamped edges is not valid, then this series will establish some criterion for the actual edge conditions.

The second series of tests will be conducted to determine systematically the influence of each of the other geometric parameters as indicated in the dimensional analysis. The number of stiffeners, skin thickness, length and radius will be varied independently. Each specimen will be tested over a wide range of pressures, thus giving the critical stress as a function of pressure for each geometric configuration.

Two major pieces of equipment are required for the cylinder test program: the test fixture itself, and a device for cutting uniform stiffeners. These two pieces of equipment are near completion.

Table 1a. Buckling Data for Conical Test Specimens Under Axial Compression ($\alpha = 0$ Degrees).

Specimen Number	$\frac{P}{t}$ (avg)	$\frac{P}{2\pi Et Z}$	$C_{exp} = \frac{P}{2\pi Et Z \cos^2 \alpha}$	C^* (Eq. 3)	$\frac{C_{exp}}{C^*}$
00.11*	400	0.300	0.300	0.247	1.22
00.12	400	0.257	0.257	0.247	1.04
00.13	400	0.241	0.241	0.247	0.98
00.14	400	0.255	0.255	0.247	1.03
00.21	533	0.229	0.229	0.222	1.03
00.22	533	0.205	0.205	0.222	0.92
00.23	533	0.229	0.229	0.222	1.03
00.31	800	0.191	0.191	0.178	1.07
00.32	800	0.191	0.191	0.178	1.07
00.33	800	0.200	0.200	0.178	1.12
00.41	1333	0.205	0.205	0.124	1.65
00.42	1333	0.195	0.195	0.124	1.57
00.43	1333	0.205	0.205	0.124	1.65
00.51	400	0.262	0.262	0.260	1.01
00.52	400	0.255	0.255	0.260	0.98
00.53	400	0.215	0.215	0.260	0.83
00.54	400	0.231	0.231	0.260	0.89
00.61	533	0.197	0.197	0.237	0.83
00.62	533	0.193	0.193	0.237	0.81
00.63	533	0.271	0.271	0.237	1.14
00.64	533	0.225	0.225	0.237	0.95
00.71	800	0.217	0.217	0.190	1.14
00.72	800	0.200	0.200	0.190	1.05
00.73	800	0.217	0.217	0.190	1.14
00.74	800	0.226	0.226	0.190	1.19
00.81	1333	0.219	0.219	0.137	1.60
00.82	1333	0.198	0.198	0.137	1.45
00.83	1333	0.188	0.188	0.137	1.37
00.84	1333	0.186	0.186	0.137	1.36
00.91	2000	0.196	0.196	0.110	1.76
00.92	2000	0.182	0.182	0.110	1.66

* Last digit refers to the specific specimens for the geometry indicated (see Reference 1 for geometry variations).

Table 1b. Buckling Data for Conical Test Specimens
Under Axial Compression ($\alpha = 10$ Degrees).

Specimen Number	$\frac{P}{t}$ (avg)	$\frac{P}{2\pi Et Z}$	$C_{exp} = \frac{P}{2\pi Et Z \cos^2 \alpha}$	C^* (Eq. 3)	$\frac{C_{exp}}{C^*}$
10.11	393	0.237	0.244	0.245	1.00
10.12	393	0.220	0.227	0.245	0.93
10.21	786	0.330	0.340	0.176	1.93
10.22	786	0.321	0.331	0.176	1.88
10.31	1310	0.261	0.269	0.125	2.15
10.32	1310	0.234	0.241	0.125	1.93
10.61	1270	0.289	0.208	0.128	2.33
10.62	1270	0.228	0.235	0.128	1.84
10.71	1515	0.257	0.265	0.123	2.15
10.72	1515	0.242	0.250	0.123	2.03

Table 1c. Buckling Data for Conical Test Specimens Under Axial Compression ($\alpha = 20$ Degrees).

Specimen Number	$\frac{P}{t}$ (avg)	$\frac{P}{2\pi Et Z}$	$C_{exp} = \frac{P}{2\pi Et Z \cos^2 \alpha}$	C^* (Eq. 3)	$\frac{C_{exp}}{C^*}$
20.11	400	0.262	0.297	0.249	1.19
20.12	400	0.244	0.276	0.249	1.11
20.21	800	0.280	0.317	0.178	1.78
20.22	800	0.266	0.301	0.178	1.69
20.31	1333	0.268	0.304	0.126	2.42
20.32	1333	0.238	0.270	0.126	2.15
20.41	2000	0.220	0.249	0.101	2.47
20.42	2000	0.211	0.239	0.101	2.37
20.51	1730	0.260	0.295	0.108	2.73
20.52	1730	0.260	0.294	0.108	2.72
20.61	1600	0.309	0.350	0.142	2.47
20.62	1600	0.297	0.336	0.142	2.37

Table 1d. Buckling Data for Conical Test Specimens Under Axial Compression ($\alpha = 30$ Degree).

Specimen Number	$\frac{P}{t}$ (avg)	$\frac{P}{2\pi Et Z}$	$C_{exp} = \frac{P}{2\pi Et \cos^2 \alpha}$	C^* (Eq. 3)	$\frac{C_{exp}}{C^*}$
30.11	405	0.247	0.329	0.252	1.31
30.12	405	0.245	0.326	0.252	1.29
30.21	810	0.215	0.286	0.180	1.59
30.22	810	0.207	0.276	0.180	1.53
30.31	1350	0.269	0.359	0.130	2.76
30.32	1350	0.263	0.350	0.130	2.69
30.41	2020	0.242	0.322	0.104	3.10
30.42	2020	0.215	0.286	0.104	2.75
30.51	1875	0.213	0.284	0.105	2.71
30.61	1430	0.188	0.250	0.123	2.03
30.62	1430	0.181	0.241	0.123	1.96
30.71	1735	0.209	0.278	0.146	1.91
30.72	1735	0.191	0.254	0.146	1.75

Table 1e. Buckling Data for Conical Test Specimens Under Axial Compression ($\alpha = 45$ Degrees).

Specimen Number	$\frac{P}{t}$ (avg)	$\frac{P}{2\pi Et Z}$	$C_{exp} = \frac{P}{2\pi Et Z \cos \alpha}$	$C^* \text{ (Eq. 3)}$	$\frac{C_{exp}}{C^*}$
45.11	406	0.182	0.364	0.251	1.45
45.12	406	0.178	0.355	0.251	1.41
45.21	812	0.185	0.370	0.180	2.06
45.22	812	0.165	0.330	0.180	1.83
45.31	1353	0.124	0.248	0.130	1.91
45.32	1353	0.113	0.226	0.130	1.74
45.41	2030	0.114	0.227	0.104	2.19
45.42	2030	0.111	0.221	0.104	2.13
45.51	1530	0.156	0.312	0.128	2.45
45.52	1530	0.153	0.306	0.128	2.40
45.61	1765	0.168	0.335	0.135	2.48
45.62	1765	0.157	0.313	0.135	2.31
45.71	1270	0.181	0.362	0.184	1.97
45.72	1270	0.179	0.357	0.184	1.94

Table 1f. Buckling Data for Conical Test Specimens Under Axial Compression ($\alpha = 60$ Degrees).

Specimen Number	$\frac{P}{t}$ (avg)	$\frac{P}{2\pi Et Z}$	$C_{exp} = \frac{P}{2\pi Et Z \cos \alpha}$	$C^* \text{ (Eq. 3)}$	$\frac{C_{exp}}{C^*}$
60.11	600	0.095	0.380	0.236	1.61
60.12	600	0.093	0.371	0.236	1.57
60.21	800	0.103	0.410	0.203	2.02
60.22	800	0.095	0.378	0.203	1.86
60.31	1200	0.093	0.373	0.158	2.36
60.32	1200	0.084	0.335	0.158	2.12
60.41	2000	0.108	0.432	0.121	3.57
60.42	2000	0.100	0.398	0.121	3.29
60.51	1300	0.084	0.335	0.157	2.13
60.52	1300	0.084	0.334	0.157	2.13
60.61	1500	0.077	0.308	0.170	1.81
60.62	1500	0.075	0.299	0.170	1.76
60.71	1200	0.126	0.503	0.189	2.66
60.72	1200	0.125	0.499	0.189	2.64

Table 2a. Buckling Data for Conical Test Specimens Under External Pressure ($\alpha = 0$ Degrees).

Specimen Number	$1 - \frac{R_1}{R_2}$	Buckling Pressure P		$\frac{P}{p}$	Number of Buckles	
		Experimental (psi)	Computed (psi)		Experimental	Computed
00.11	0	0.1010	0.1086	0.93	6	9
00.12	0	0.0990	0.1086	0.91	6	9
00.21	0	0.0537	0.0523	1.03	7	9
00.22	0	0.0443	0.0523	0.85	7	9
00.31	0	0.0198	0.0189	1.05	8	10
00.32	0	0.0184	0.0189	0.97	8	10
00.41	0	0.0058	0.0053	1.10	9	12
00.42	0	0.0054	0.0053	1.03	9	12
00.51	0	0.1830	0.2179	0.84	10	12
00.52	0	0.2230	0.2179	1.02	10	12
00.61	0	0.1093	0.1059	1.03	9	12
00.62	0	0.1194	0.1059	1.13	11	13
00.71	0	0.0344	0.0382	0.90	11	13
00.72	0	0.0366	0.0382	0.96	11	14
00.81	0	0.0108	0.0106	1.02	12	14
00.82	0	0.0101	0.0106	0.95	13	16
00.83	0	0.0101	0.0106	0.95	13	16
00.84	0	0.0098	0.0106	0.93	13	16
00.85	0	0.0095	0.0106	0.89	13	16
00.86	0	0.0106	0.0106	1.00	13	16

Table 2b. Buckling Data for Conical Test Specimens Under External Pressure ($\alpha = 10$ Degrees).

Specimen Number	$1 - \frac{R_1}{R_2}$	Buckling Pressure \bar{P}		$\frac{P}{\bar{P}}$	Number of Buckles	
		Experimental (psi)	Computed (psi)		Experimental	Computed
10.11	0.45	0.0740	0.0683	1.08	5	6-7
10.12	0.45	0.0690	0.0683	1.03	5	6-7
10.21	0.45	0.0117	0.0119	0.98	6	7-8
10.22	0.45	0.0125	0.0119	1.05	6	7-8
10.31	0.45	0.0035	0.0033	1.05	7	8-9
10.32	0.45	0.0034	0.0031	1.03	7	8-9
10.41	0.45	0.0011	0.0012	0.89	7	8-9
10.42	0.45	0.0010	0.0012	0.87	7	9-10
10.51	0.70	0.0009	0.0010	0.89	5	9-10
10.52	0.70	0.0009	0.0010	0.89	5	6-7
10.61	0.50	0.0037	0.0032	1.17	5	6-7
10.62	0.50	0.0034	0.0032	1.07	7	7-8
10.71	0.20	0.0058	0.0053	1.07	7	7-8
10.72	0.20	0.0060	0.0053	1.14	13	13-14
					12	13-14

Table 2c. Buckling Data for Conical Test Specimens Under External Pressure ($\alpha = 20$ Degrees).

Specimen Number	$1 - \frac{R_1}{R_2}$	Buckling Pressure		$\frac{p}{\bar{p}}$	Number of Buckles	
		P Experimental (psi)	\bar{p} Computed (psi)		Experimental	Computed
20.11	0.50	0.1240	0.1173	1.06	7	8-9
20.12	0.50	0.1130	0.1173	0.96	7	8-9
20.21	0.50	0.0178	0.0207	0.86	9	10-11
20.22	0.50	0.0202	0.0207	0.98	9	10-11
20.31	0.50	0.0055	0.0057	0.96	10	11-12
20.32	0.50	0.0056	0.0057	0.98	10	11-12
20.41	0.50	0.0017	0.0021	0.81	11	12-13
20.42	0.50	0.0021	0.0021	1.02	11	12-13
20.51	0.70	0.0018	0.0019	0.99	7	9-10
20.52	0.70	0.0019	0.0019	1.05	7	9-10
20.61	0.20	0.0114	0.0111	1.03	16	20-21
20.62	0.20	0.0103	0.0111	0.92	16	20-21

Table 2d. Buckling Data for Conical Test Specimens Under External Pressure ($\alpha = 30$ Degrees).

Specimen Number	$\frac{R_1}{1 - R_2}$	P Experimental (psi)	Buckling Pressure \bar{P}		$\frac{P}{\bar{P}}$	Number of Buckles	
			Experimental (psi)	Computed (psi)		Experimental	Computed
30.11	0.60	0.1375	0.1375	0.1412	0.97	7	8-9
30.12	0.60	0.1550	0.1550	0.1412	1.10	7	8-9
30.13	0.60	0.1300	0.1300	0.1412	0.92	7	8-9
30.14	0.60	0.1480	0.1480	0.1412	1.05	7	8-9
30.21	0.60	0.0232	0.0232	0.0248	0.94	8	10-11
30.22	0.60	0.0221	0.0221	0.0248	0.89	8	10-11
30.23	0.60	0.0224	0.0224	0.0248	0.90	8	10-11
30.31	0.60	0.0072	0.0072	0.0069	1.04	8	12-13
30.32	0.60	0.0068	0.0068	0.0069	0.99	8	12-13
30.41	0.60	0.0021	0.0021	0.0025	0.85	11	13
30.42	0.60	0.0023	0.0023	0.0025	0.92	11	13
30.51	0.70	0.0024	0.0024	0.0025	0.96	8	11-12
30.52	0.70	0.0024	0.0024	0.0025	0.96	8	11-12
30.61	0.50	0.0076	0.0076	0.0077	0.98	11	13-14
30.62	0.50	0.0077	0.0077	0.0077	1.00	11	13-14
30.71	0.20	0.0136	0.0136	0.0111	1.23	21	20-21
30.72	0.20	0.0140	0.0140	0.0111	1.26	21	20-21

Table 2e. Buckling Data for Conical Test Specimens Under External Pressure ($\alpha = 45$ Degrees).

Specimen Number	$1 - \frac{R_1}{R_2}$	Buckling Pressure		$\frac{P}{\bar{P}}$	Number of Buckles	
		Experimental (psi)	Computed (psi)		Experimental	Computed
45.11	0.85	0.1370	0.1403	0.98	6	7
44.12	0.85	0.1400	0.1403	1.00	6	7
45.21	0.85	0.0259	0.0247	1.05	8	8-9
45.22	0.85	0.0240	0.0247	0.97	8	8-9
45.31	0.85	0.0063	0.0069	0.91	10	9-10
45.32	0.85	0.0066	0.0069	0.96	10	9-10
45.41	0.85	0.0025	0.0025	1.00	9	10-11
45.42	0.85	0.0026	0.0025	1.06	10	10-11
45.51	0.70	0.0076	0.0069	1.09	9	11-12
45.52	0.70	0.0074	0.0069	1.07	9	11-12
45.61	0.50	0.0071	0.0070	0.90	13	14-15
45.62	0.50	0.0076	0.0079	0.96	12	14-15
45.71	0.20	0.0500	0.0582	0.86	20	22-23
45.72	0.20	0.0465	0.0582	0.80	21	22-23

Table 2f. Buckling Data for Conical Test Specimens Under External Pressure ($\alpha = 60$ Degrees).

Specimen Number	$1 - \frac{R_1}{R_2}$	Buckling Pressure		$\frac{P}{\bar{P}}$	Number of Buckles	
		P Experimental (psi)	\bar{P} Computed (psi)		Experimental	Computed
60.11	0.80	0.0940	0.1029	0.91	7	7-8
60.12	0.80	0.0940	0.1029	0.91	7	7-8
60.21	0.80	0.0468	0.0499	0.74	6	8
60.22	0.80	0.0476	0.0499	0.98	6	8
60.31	0.80	0.0173	0.0180	0.96	8	9
60.32	0.80	0.0176	0.0180	0.98	8	9
60.41	0.80	0.0045	0.0050	0.91	10	10-11
60.42	0.80	0.0053	0.0050	1.05	10	10-11
60.51	0.70	0.0162	0.0184	0.88	8	10
60.52	0.70	0.0165	0.0184	0.90	9	10
60.61	0.50	0.0194	0.0213	0.91	10	13-14
60.62	0.50	0.0188	0.0213	0.83	10	13-14

REFERENCES

1. Lutwak, S. "Semiannual Report on Development of Design Criteria for Elastic Instability of Thin Shell Structures, 1 January 1951 to 30 June 1959." STL Report No. TR-59-0000-00715.
2. Johnson, H. W. STL Report No. 61.1-190, "Development of Design Criteria for Elastic Instability of Thin-Shell Structures," February 1959.
3. Lundquist, E. E. and E. H. Schuette. "Strength of Thin-Wall Truncated Cones of Circular Section." NACA Wartime Report L-492, 1942.
4. Homewood, R. H., A. C. Brine and A. E. Johnson. "Buckling Instability of Monocoque Shells." Avco Technical Report RAD-TR-9-59-20, August 1959.
5. Seide, P. "On the Buckling of Truncated Conical Shells Under Uniform Hydrostatic Pressure." STL Report No. TR-59-0000-00684, June 1959. AD - 219504
6. Batdorf, S. B. "A Simplified Method of Elastic-Stability Analysis for Thin Cylindrical Shells." NACA TR 874, 1947.
7. Bowie, O. A., B. S. Parker, P. P. Radkowski and J. I. Bluhm. "A Study of the IRBM (Jupiter) Bulkheads." Watertown Arsenal Laboratories Report No. 880-54, August 1956.
8. Seide, P. "Compressive Buckling of Longitudinally Stiffened Circular Cylinders." Report No. AM6-11, GMRD, Ramo-Wooldridge Corporation, 31 May 1956.
9. Peterson, J. P. and M. B. Dow. "Compression Tests on Circular Cylinders, Stiffened Longitudinally by Closely Spaced Z-Section Stringers." NASA Memorandum, 2-12-59L, March 1959.
10. Rafel, N. and C. W. Sandkin, Jr. "Effects of Normal Pressure on the Critical Compressive and Shear Stress of Curved Sheets." NACA Wartime Report L-57, March 1945.
11. Sechler, E. E. and L. G. Dunn. "Airplane Structural Analysis and Design." Wiley and Sons, Inc., 1942, p. 316.
12. Rafel, N. "Effects of Normal Pressure on the Critical Compressive Stress of Curved Sheets." NACA Wartime Report, L-258, November 1942.
13. Lo, H., H. Crate and E. B. Schwartz. "Buckling of Thin Walled Cylinders Under Axial Compression and Internal Pressure." NACA Report 1027, 1951.

14. Fung, Y. C. and E. E. Sechler. "Buckling of Thin Walled Circular Cylinders Under Axial Compression and Internal Pressure." *Journal of the Aeronautical Sciences*, May 1957, pp. 351-356.
15. Harris, L. A., H. S. Suer, W. T. Skene and R. J. Benjamin. "The Stability of Thin Walled Unstiffened Circular Cylinders Under Axial Compression Including the Effects of Internal Pressure." *Journal of the Aeronautical Sciences*, Vol. 24, No. 8, August 1957, pp. 587-596.

DISTRIBUTION

E. A. Adler (5)	H. R. Lawrence
M. V. Barton (6)	D. W. McNabb
J. G. Berry (20)	R. F. Mettler
J. F. Bricca	E. J. Morgan
F. M. Brown	R. E. Moulton
R. A. Burgin	J. E. Peterson
J. F. Chalmers	D. N. Pitts
A. F. Donovan	P. Seide
R. B. Dreizler	R. O. Shepard
W. M. Duke	R. Slaney
L. G. Dunn	L. A. Snodgrass (2)
D. L. Forbes (22 + 1 reproducible)*	G. E. Solomon
F. W. Hesse	F. C. Thurston (2)
W. S. Hotchkiss	W. C. Tracey
H. W. Johnson (6)	V. I. Weingarten
A. Kaplan (20)	STL Library (5)
Z. Kohlmeyer	

* Includes 21 copies plus one reproducible for transmittal to WDAT.

UNCLASSIFIED

UNCLASSIFIED